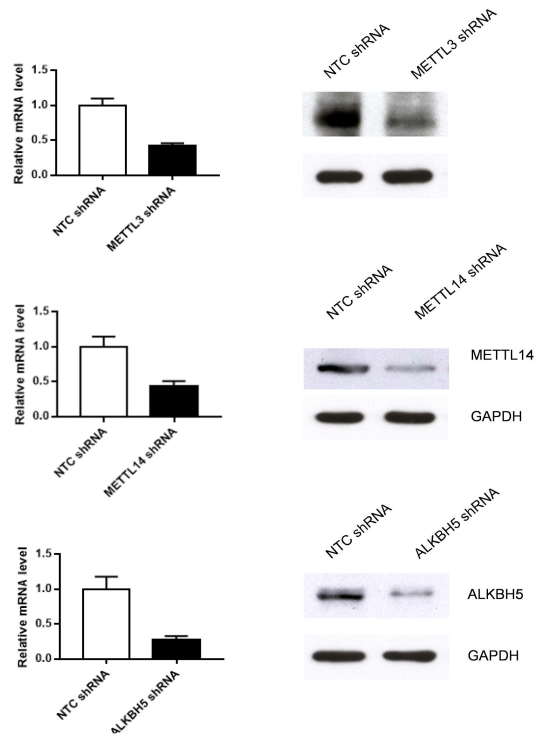
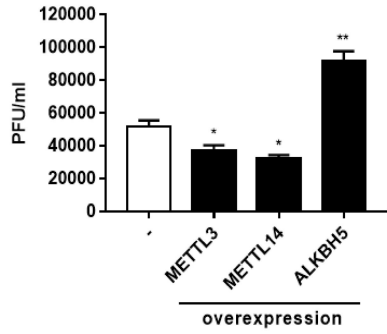
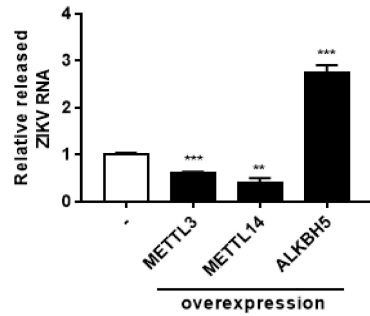
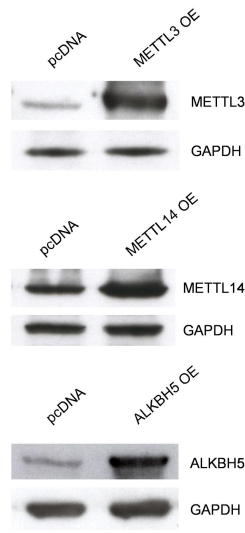
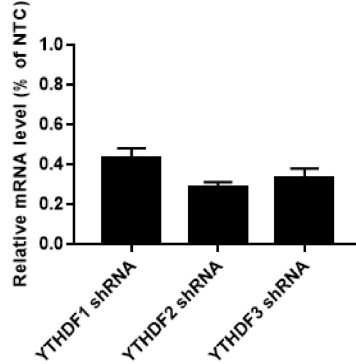
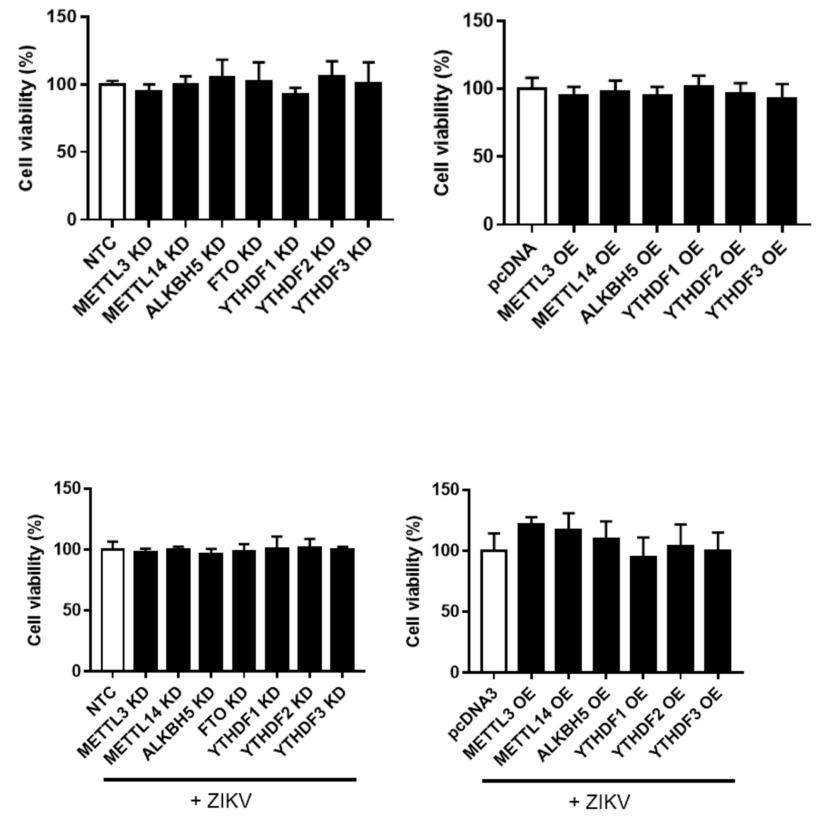
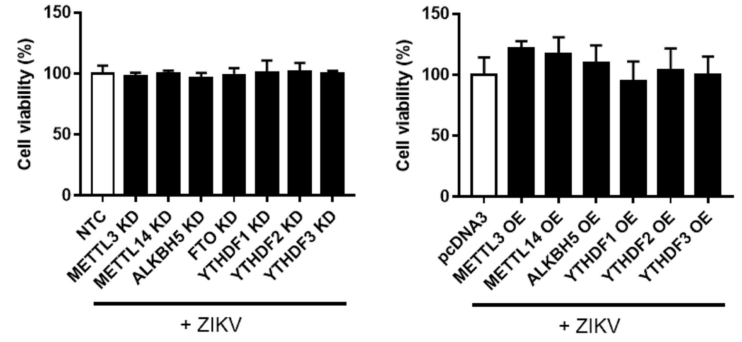


A**B****C****D****E****F****G**

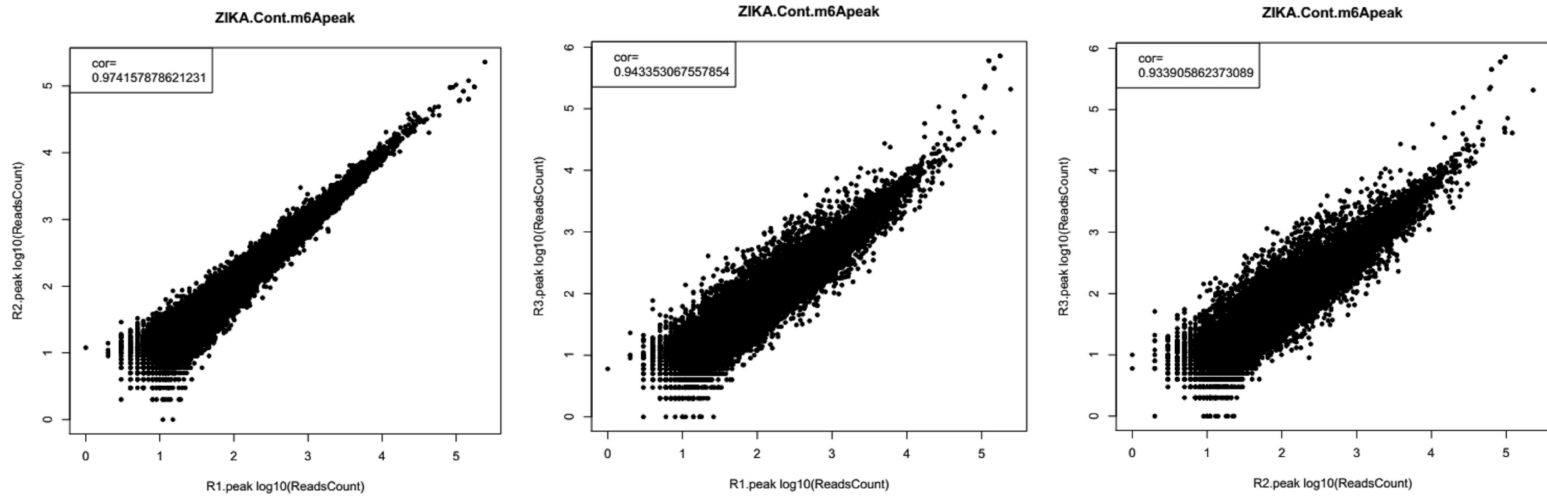
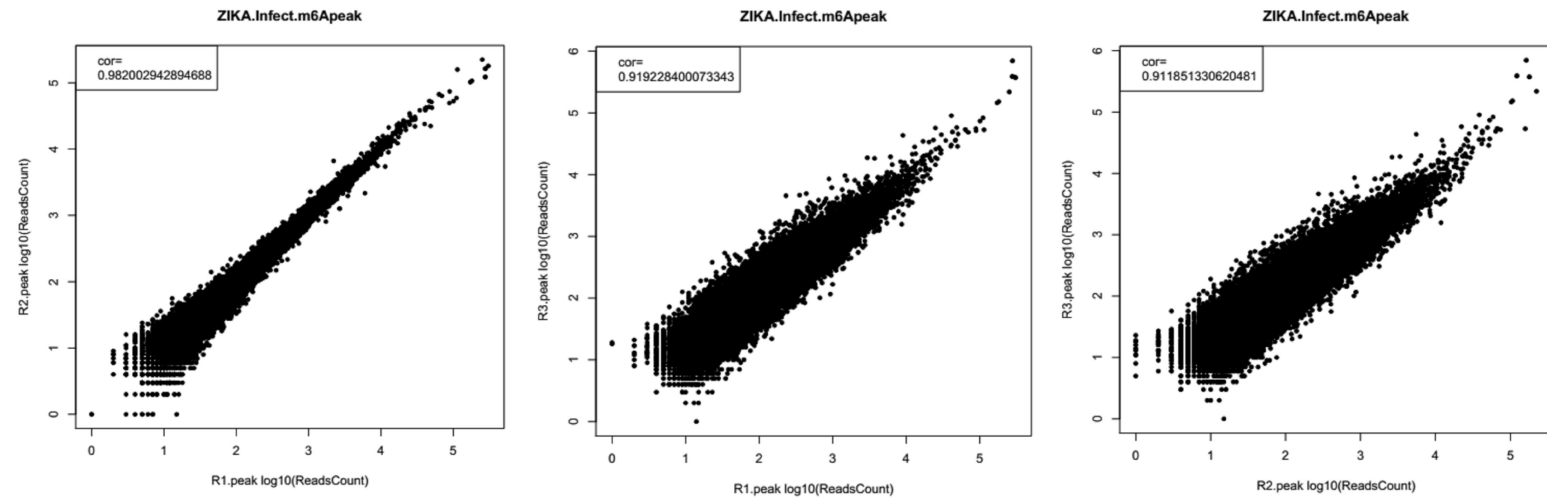
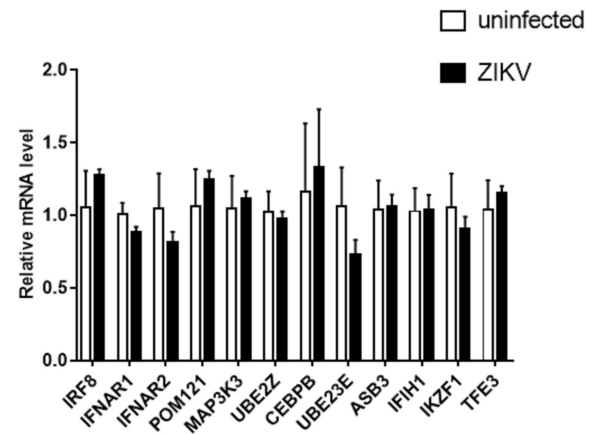
A**B****C**

Figure S1. Related to Figure 1

(A) Correlation test between two biological replicates of vgRNA is shown.

(B) Alignment and m⁶A motif identity/conservation is shown for the 12 m⁶A peaks identified in ZIKV RNA among five ZIKV strains (MR766, Paraiba, KX156774, KU501215 and FSS13025). The DRACH, MGACK, and UGAC consensus motifs are highlighted in yellow.

(C) Nuclear and cytoplasmic localization of METTL3, METTL14 and ALKBH5 visualized by immunostaining of uninfected (Mock) and ZIKV-infected 293T cells at 24 h after infection. Cells were counterstained with DAPI. Scale bar, 100 μm. Arrows indicate cells with evident cytoplasmic localization of the indicated protein.

Figure S2. Related to Figure 2

(A) Silencing efficiency of shRNAs. METTL3, METTL14, and ALKBH5 expression in 293T cells expressing non-targeting shRNA (NTC) or the indicated gene-specific shRNAs, analyzed by qRT-PCR (left) or western blotting (right). N = 3.

(B, C) Viral titers (particle production) (B) and ZIKV RNA levels in supernatants (C) of 293T cells overexpressing METTL3, METTL14, or ALKBH5 proteins. N = 3.

(D) Western blot analysis of METTL3, METTL14, and ALKBH5 proteins in 293T cells expressing control pcDNA or the indicated overexpression vectors. GAPDH was probed as a loading control. All data are the mean ± SEM of the indicated number of replicates. Student's t-test * p < 0.05, ** p < 0.005, *** p < 0.0005.

(E) Silencing efficiency of YTHDF1, 2, and 3 expression in 293T cells expressing indicated gene-specific shRNAs or non-targeting shRNA control (NTC) analyzed by qRT-PCR.

(F, G) Cell viability analyses by MTS assays in uninfected (F) and ZIKV infected (G) for specific shRNA knockdown (KD) or overexpression (OE) experiments as indicated.

Figure S3. Related to Figure 3

(A,B) Paired correlation analysis of the three biological replicates of (A) uninfected (control R1, R2, R3) and (B) ZIKV-infected samples (infect R1, R2, R3). Each paired results exhibit high correlation values, indicating good replicability.

(C) Relative mRNA level of genes listed in Suppl. Table 1 in mock or ZIKV-infected cells quantified by qRT-PCR.

Table S1, related to Fig 3 | Immune-Related Genes with Newly Gained or Lost m⁶A Peaks in ZIKV-Infected Cells

ZIKV-enriched m⁶A genes - Immunity related	
Gene	New m6A peak location
CREBBP	CDS
NCAM1	CDS
CLTC	CDS
KPNA2	CDS
IRF2	CDS
PML	CDS
IRF8	3'_UTR_junction
IFNAR2	3'_UTR
IFNAR1	3'_UTR
POM121	3'_UTR
SH2B1	CDS
IRS1	CDS
MAP3K3	3'_UTR
KIF3C	CDS
HUWE1	CDS
UBE2E3	5'_UTR_junction
UBE2Z	3'_UTR
TRIM9	5'_UTR
UBR2	CDS
ASB3	5'_UTR
DZIP3	CDS
TAP2	CDS
AP1M1	CDS
DYNC1L12	CDS
RAP1GAP2	CDS
IFIH1	5'_UTR
APP	CDS
C4A	CDS
CEBPB	3'_UTR_junction
IKZF1	5'_UTR
TFE3	5'_UTR_junction
CACTIN	CDS
WNT5A	CDS
CSF1	CDS
ZBTB46	CDS
BMP4	CDS
PARP1	CDS
C4B	CDS
SUSD4	CDS

ZIKV-depleted m⁶A genes - Immunity related	
Gene	Lost m6A peak location
TYRO3	Exon_junction
GLI2	CDS
PATZ1	CDS
HMGB2	Exon_junction
ITGB1	Exon_junction
MOV10	CDS
RFWD3	Exon_junction
LRRC8A	CDS
MYLK	Exon_junction
HMGB2	Exon_junction
GLI2	CDS
SH3D19	Exon_junction
TACC3	CDS
ACTR1A	5'_UTR_junction
SNRPB	5'_UTR
KIF15	5'_UTR
CD24	5'_UTR
CD24	5'_UTR
PAK1	3'_UTR
MMP14	3'_UTR
ERCC1	3'_UTR
BRK1	3'_UTR
ERCC1	3'_UTR
BRK1	3'_UTR
SP3	CDS
RPS6KB2	Exon_junction
IRS2	CDS
MAFB	CDS
ERCC2	Exon_junction
LIG4	CDS
NFKB1	Exon_junction
CHD2	CDS
KAT6A	CDS
NFKB1	Exon_junction
AGO4	Exon_junction
IRS2	CDS
ERCC2	Exon_junction
ONECUT1	5'_UTR_junction
SEC24C	5'_UTR_junction

SUPPLEMENTAL EXPERIMENTAL PROCEDURES

Lentiviral Preparation, Cell Transduction, and Viral RNA Quantification

293T cells (10^6) were transfected with pLKO shRNA (1 μ g), psPAX.2 (0.75 μ g), and pMD2.G (0.25 μ g) vectors using Lipofectamine 2000 and Opti-MEM (Invitrogen) according to the manufacturer's instructions. The medium was replaced with complete DMEM at 4 h post-transfection, and 48 h later, the supernatant was collected, filtered through a 0.22 μ m membrane, and incubated with 293T cells in the presence of 1 μ g/ml polybrene. After 12 h, the medium was removed and replaced with complete DMEM. At 3 days post-transduction, 293T cells were infected with MR766 virus at an MOI of 5. After 12 h, the medium was changed. Viral supernatants were collected and total cellular RNA was prepared at 48 h after infection. Viral titer was assessed as described above. Total RNA was extracted using TRIzol reagent (Invitrogen). mRNA expression was measured using iScript Reverse Transcription Supermix for RT-qPCR and iTaq Universal SYBR Green Supermix (Bio-Rad) for qPCR. Viral RNA released into the supernatant was measured using an iScript One Step RT-PCR kit.

Plaque-Forming Unit Assay

Confluent Vero cells were inoculated with four serial 10-fold dilutions of supernatants from infected cells. After 2 h, the cells were washed, overlaid with plaque medium containing 0.4% agarose, and cultured at 37°C for 4 days. Cells were then fixed with 3.7% formaldehyde, stained with 0.1% crystal violet in 20% ethanol, and plaques counted.

METTL3, METTL14, and ALKBH5 Overexpression

METTL3, METTL14, and ALKBH5 overexpression plasmids were constructed by cloning the corresponding cDNAs into the mammalian expression vector pcDNA3 (Invitrogen). 293T cells were transfected using Lipofectamine 2000 and Opti-MEM. The medium was replaced with complete DMEM after 4 h, and 48 h later, the cells were infected with MR766 virus at an MOI of 5. Viral supernatants were collected and total cellular RNA was prepared at 24 h post-infection. Viral titer and RNA were quantified as described above.

FLAG-YTHDF1-3 Overexpression and Immunoprecipitation

293T cells (2×10^6) were transfected with 2 μ g FLAG-YTHDF or control pcDNA plasmids using Lipofectamine 2000 and Opti-MEM. After 4 h, the medium was replaced with complete DMEM, and 20 h later, the cells were infected with ZIKV at an MOI of 5. At 24 h post-infection, cells

were lysed with Pierce IP lysis buffer supplemented with protease inhibitors and RNaseOUT. An aliquot of cleared lysate (5%) was saved as input. The remaining lysate was incubated overnight at 4°C with 2 µg of anti-FLAG antibody (clone M2, Sigma) and 50 µl of Protein G Dynabeads (Invitrogen). Beads were washed three times with lysis buffer and divided in half for RNA extraction and RT-qPCR analysis or for western blot analysis.

Liquid Chromatography–Tandem Mass Spectrometry

Genomic RNA from MR766 ZIKV was isolated from Vero cells as described previously (Dang et al., 2016), and modified nucleoside levels were quantified using LC-MS/MS as described (Jia et al., 2011). Briefly, 50 ng of viral genomic RNA was digested by nuclease P1 (2 U, Wako) in 25 µl of buffer containing 25 mM NaCl and 2.5 mM ZnCl₂ at 42°C for 2 h, and then NH₄HCO₃ (1 M, 3 µl) and alkaline phosphatase (0.5 U, Sigma) were added and the samples were incubated at 37°C for an additional 2 h. The samples were diluted to 50 µl with nuclease-free water, filtered (0.22 µm pore size, 4 mm diameter, Millipore), and 10 µl aliquots were taken for analysis.

Nucleosides were separated on a reverse phase ultra-performance liquid chromatography C18 column with in-line mass spectrometry detection using an Agilent 6410 QQQ triple-quadrupole LC mass spectrometer in positive electrospray ionization mode. Each modified nucleoside was quantified by the ratio of modified to unmodified nucleoside levels.

Data Analysis

For data analysis, after removing the adapter, the reads were mapped to human genome (hg38) and ZIKA genome (NC_012532) by using Tophat2 (Kim et al., 2013). The peak calling method was modified from the published method (Dominissini et al., 2012). To call m⁶A peaks, the longest isoform of each Human RefSeq gene (and the whole genome of ZIKV) was scanned using a 100 bp sliding window with 10 bp steps. To reduce bias from potential inaccurate gene structure annotation and the arbitrary use of the longest isoform, windows with read counts less than 1/20 of the top window in both m⁶A immunoprecipitate and input samples were excluded. For each gene, the read count in each window was normalized by the median count of all windows of that gene. A negative binomial model was used to identify the differential windows between immunoprecipitate and input samples by using the edgeR package (Robinson et al., 2010), for each and eventually combining information from all three replicates in the two groups. The window was called as positive if the FDR was <1% and the log₂(enrichment score) was ≥1. Overlapping positive windows were merged. The following were calculated to obtain the enrichment score of each peak (or window): (a) read counts of the immunoprecipitated sample

in the current peak/window, (b) median read counts of the immunoprecipitated sample in all 100 bp windows on the current mRNA, (c) read counts of the input sample in the current peak/window, and (d) median read counts of the input sample in all 100 bp windows on the current mRNA. The enrichment score of each window was calculated as $([a \times d])/([b \times c])$.

Primer List

Primer	Sequence
GAPDH Fwd	TGGCGGGGAAGTCAG
GAPDH Rev	CGGAGGAGAAATCGGGC
ZIKV Fwd	TTGGTCATGATACTGCTGATTGC
ZIKV Rev	CCCTCCACGAAGTCTCTATTGC
METTL3 Fwd	GACACGTGGAGCTCTATCCA
METTL3 Rev	GGAAGGTTGGAGACAATGCT
METTL14 Fwd	TCCCAAATCTAAATCTGACCG
METTL14 Rev	CTCTAAAGCCACCTCTTTCTC
ALKBH5 Fwd	AGGGACCCTGCTCTGAAAC
ALKBH5 Rev	TCCTTGTCATCTCCAGGAT

shRNA Sequences

shRNA	Sequence
NTC	CCGCAGGTATGCACGCGT
METTL3-1	CCGGGCAAGTATGTTCACTATGAAACTCGAGTTTCATAGTGAACA TACTTGCTTTTTG
METTL3-2	CCGGGCCAAGGAACAATCCATTGTTCTCGAGAACAATGGATTGT TCCTTGGCTTTTTG
METTL14-1	CCGGCCATGTACTIONACAAGCCGATACTCGAGTATCGGCTTGTA GTACATGGTTTT
METTL14-2	CCGGGCCGTGGACGAGAAAGAAATACTCGAGTATTTCTTTCTCG TCCACGGCTTTTT
ALKBH5-1	CCGGGAAAGGCTGTTGGCATCAATACTCGAGTATTGATGCCAAC AGCCTTTCTTTTTG
ALKBH5-2	CCGGCCACCCAGCTATGCTTCAGATCTCGAGATCTGAAGCATAG CTGGGTGGTTTTTG
FTO-1	CCGGCGGTTCAACCTCGGTTTAGCTCGAGCTAAACCGAGGTT GTGAACCGTTTTTG
FTO-2	CCGGTCACCAAGGAGACTGCTATTTCTCGAGAAATAGCAGTCTC CTTGGTGATTTTTG
YTHDF1-1	CCGGCCCTACCTGTCCAGCTATTACCTCGAGGTAATAGCTGGAC AGGTAGGGTTTTTG
YTHDF1-2	CCGGCCCGAAAGAGTTTGAGTGGAACCTCGAGTTCCACTCAA CTTTCCGGGTTTTTG
YTHDF2-1	CCGGGCTACTCTGAGGACGATATTCCTCGAGGAATATCGTCCTC AGAGTAGCTTTTTG
YTHDF2-2	CCGGCGGTCCATTAATAACTATAACCTCGAGGTTATAGTTATTAA TGGACCGTTTTTG
YTHDF3-1	CCGGTAAGTCAAAGAAGACGTATTACTCGAGTAATACGTCTTCTT TGACTTATTTTTG
YTHDF3-2	CCGGGAAGTCTGTTGTGGACTATAACTCGAGTTATAGTCCACAA CAGACTTCTTTTTG

SUPPLEMENTAL REFERENCES

Dang, J., Tiwari, S.K., Lichinchi, G., Qin, Y., Patil, V.S., Eroshkin, A.M., and Rana, T.M. (2016). Zika Virus Depletes Neural Progenitors in Human Cerebral Organoids through Activation of the Innate Immune Receptor TLR3. *Cell Stem Cell* 19, 258-265.

Dominissini, D., Moshitch-Moshkovitz, S., Schwartz, S., Salmon-Divon, M., Ungar, L., Osenberg, S., Cesarkas, K., Jacob-Hirsch, J., Amariglio, N., Kupiec, M., *et al.* (2012). Topology of the human and mouse m6A RNA methylomes revealed by m6A-seq. *Nature* 485, 201-206.

Jia, G., Fu, Y., Zhao, X., Dai, Q., Zheng, G., Yang, Y., Yi, C., Lindahl, T., Pan, T., Yang, Y.G., *et al.* (2011). N6-methyladenosine in nuclear RNA is a major substrate of the obesity-associated FTO. *Nature chemical biology* 7, 885-887.

Kim, D., Pertea, G., Trapnell, C., Pimentel, H., Kelley, R., and Salzberg, S.L. (2013). TopHat2: accurate alignment of transcriptomes in the presence of insertions, deletions and gene fusions. *Genome Biol* 14, R36.

Robinson, M.D., McCarthy, D.J., and Smyth, G.K. (2010). edgeR: a Bioconductor package for differential expression analysis of digital gene expression data. *Bioinformatics* 26, 139-140.